Polar Geosci., 11, 32-41, 1998

AN INTRAPLATE EARTHQUAKE THAT OCCURRED NEAR SYOWA STATION, EAST ANTARCTICA

Hiroaki NEGISHI[1], Yoshifumi NOGI[2] and Katsutada KAMINUMA[2]

[1] *Research Center for Earthquake Prediction, Disaster Prevention Research Institute, Kyoto University, Gokasho, Uji 611-0011*
[2] *National Institute of Polar Research, Kaga 1-chome, Itabashi-ku, Tokyo 173-8515*

Abstract: An intraplate earthquake with m_b 4.6 occurred offshore of the Prince Olav Coast, East Antarctica on September 25, 1996. This earthquake was the biggest and the first one to be located within 500 km of Syowa Station (69.0° S, 39.6° E) in the past four decades since seismic observations started under the IGY in 1957. The event was recorded by the broadband seismometers at Syowa Station and Mawson Station (67.6° S, 62.9° E), Antarctica. The moment tensor solution of this event was determined using the waveform inversion technique. The source mechanism indicates north-south compressional strike-slip faulting wih little dip-slip component. A straightforward grid search was applied to the data to evaluate the uniqueness of the solution. The minimum error was obtained for close strike, dip and rake angles that obtained in the inversion, so it can be said that the inversion result is suitable. The earthquake occurred on the gravitational lineament regarded as a fracture zone with NW-SE linear trend. The resultant mechanism has a faulting plane with a strike parallel to the fracture zone. Thus, this earthquake might be a fracturing along the pre-existed lineament inside the Antarctic plate.

key words: intraplate earthquake, broadband seismogram, moment tensor inversion, gravity lineament

1. Introduction

Since the initiation of the International Geophysical Year (IGY) in 1957, seismological observations have been continuously undertaken by Japan and some other countries in and around the Antarctic Continent. The main purpose of the observations is the recording of waveforms from worldwide teleseisms. Previous studies have reported the existence of local earthquakes located around Syowa Station (*e.g.* KAMINUMA, 1994), however their activities have been very low. Figure 1 shows the epicenter distribution of earthquakes in and around the Antarctic Continent from 1904 to 1991 determined by the International Seismological Center with some modifications by KAMINUMA (1994). The seismic activity is generally concentrated along the boundary of the Antarctic plate and at the tip of the Antarctic Peninsula. Among the earthquakes on the Antarctic Continent, there have been only seven tectonic events with magnitude larger than 4.0 since IGY (Fig. 2). The intraplate seismic activity is very low, but the magnitude of the some intraplate earthquakes is larger than 6.0. Since the compilation of intraplate seismicity in the Antarctic plate over a period of 55 years,

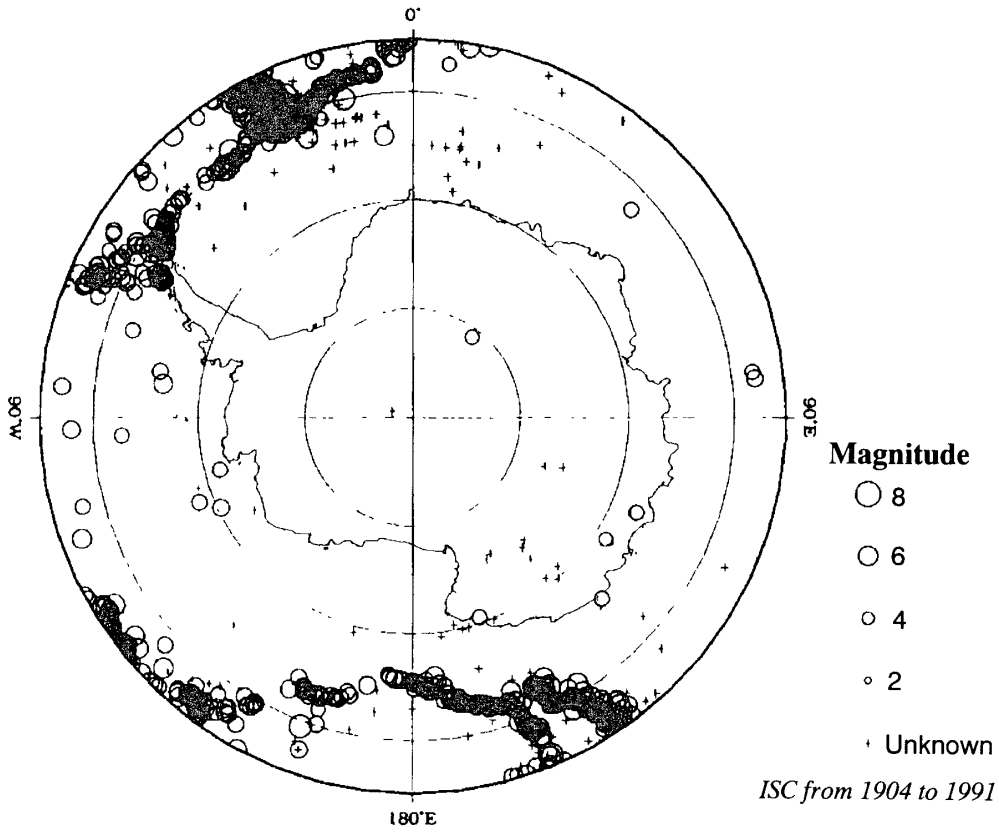

Fig. 1. Earthquake locations in the Antarctic region determined by the International Seismological Center from 1904 to 1991 (after KAMINUMA, *1994).*

OKAL (1981) concluded that the intraplate seismicity of Antarctica is comparable to that of other continent-bearing, slow-moving plates, such as Africa.

An earthquake with *S-P* time of 41.5 s was recorded at Syowa Station at 1500 (UT) on 25 September 1996. The event was identified as a nearby earthquake from its waveform and duration. Soon afterward, from E-mail information provided by the Quick Epicenter Determination (managed by the United States Geological Survey), the event was located offshore of Enderby Land as an intraplate earthquake. The area is about 420 km northeast of Syowa Station.

This is the first intraplate earthquake located near Syowa Station with magnitude larger than 4.0. Therefore, the determination of its focal mechanism is very important to understand the stress field around Syowa Station. As the earthquake was recorded at only few stations of the world wide network, the mechanism of this earthquake cannot be determined by using some existing methods like the *P*-wave first motion analysis or the moment tensor inversion of teleseismic records (*e.g.* KIKUCHI and KANAMORI, 1991).

Recently, KOSUGA (1996) succeeded in moment tensor determination for the small to moderate earthquakes by using broadband data with local to regional distances from an epicenter. In this technique, *P*-wave, *S*-wave and surface wave as well as the near-field term from the local to regional events are analyzed. The moment tensor solution can be determined using only a single station with *a priori* hypocentral parameters. In the case of the 25 September 1996 event, the solution was obtained by

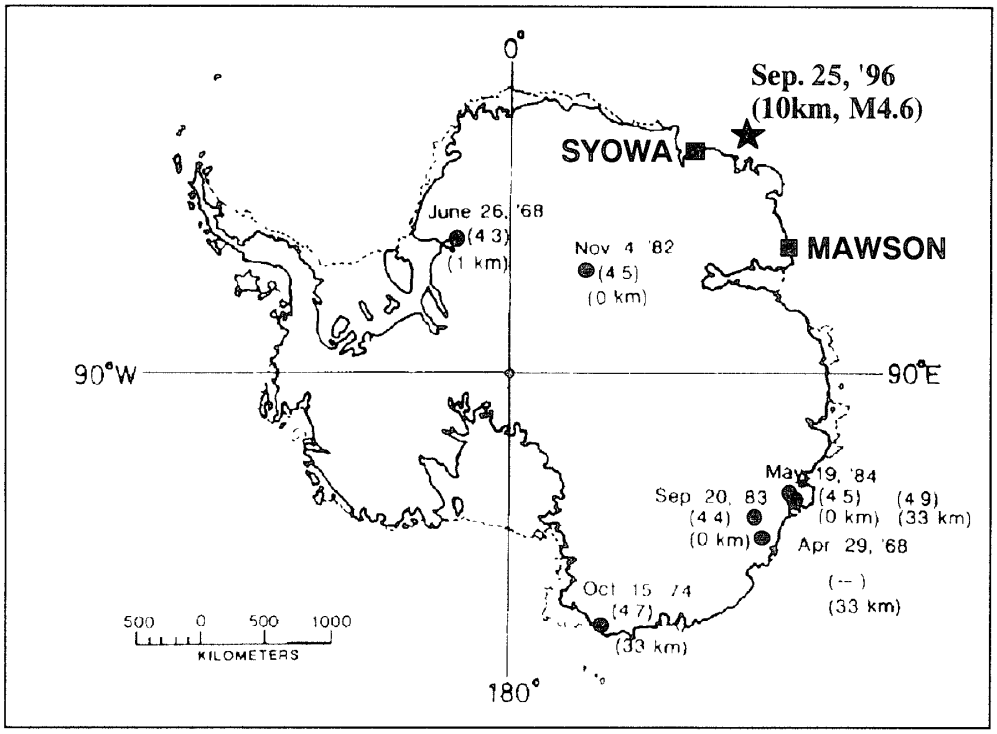

Fig. 2. Distribution of the intraplate earthquakes on the Antarctic continent since 1960. The focal depths and body-wave magnitudes of the events are also shown in the brackets. A solid star indicates the location of the 1996 event, and solid squares indicate the position of Syowa Station (operated by Japan) and Mawson Station (Australia) (revised from KAMINUMA, 1994).

adopting Kosuga's technique for the broadband data recorded at Syowa (69.01°S, 39.59°E) and Mawson (67.60°S, 62.87°E) Stations.

2. Data and Analysis

2.1. Hypocenter and waveform used in this study

The hypocentral parameters were reported on the Preliminary Determination of Epicenters (PDE) determined by the National Earthquake Information Center (NEIC) as follows:

Origin time:	25 September 1996	1459:50.1 (UTC)
Latitude:	65.637°S	
Longitude:	44.382°E	
Depth:	10 km	
Magnitude:	m_b 4.6.	

The epicenter is located about 420 km northeast of Syowa Station (Fig. 2). The depth of the ocean floor in this area is 3500–4000 m.

The three-component waveform data obtained at Syowa Station and Mawson Station were used for the moment tensor inversion. The locations of these stations are shown in Fig. 2. The seismometers are STS-1 (WIELANDT and STRECKEISEN, 1982) at Syowa Station and CMG-3 (Güralp System, LTD.) at Mawson Station, respectively.

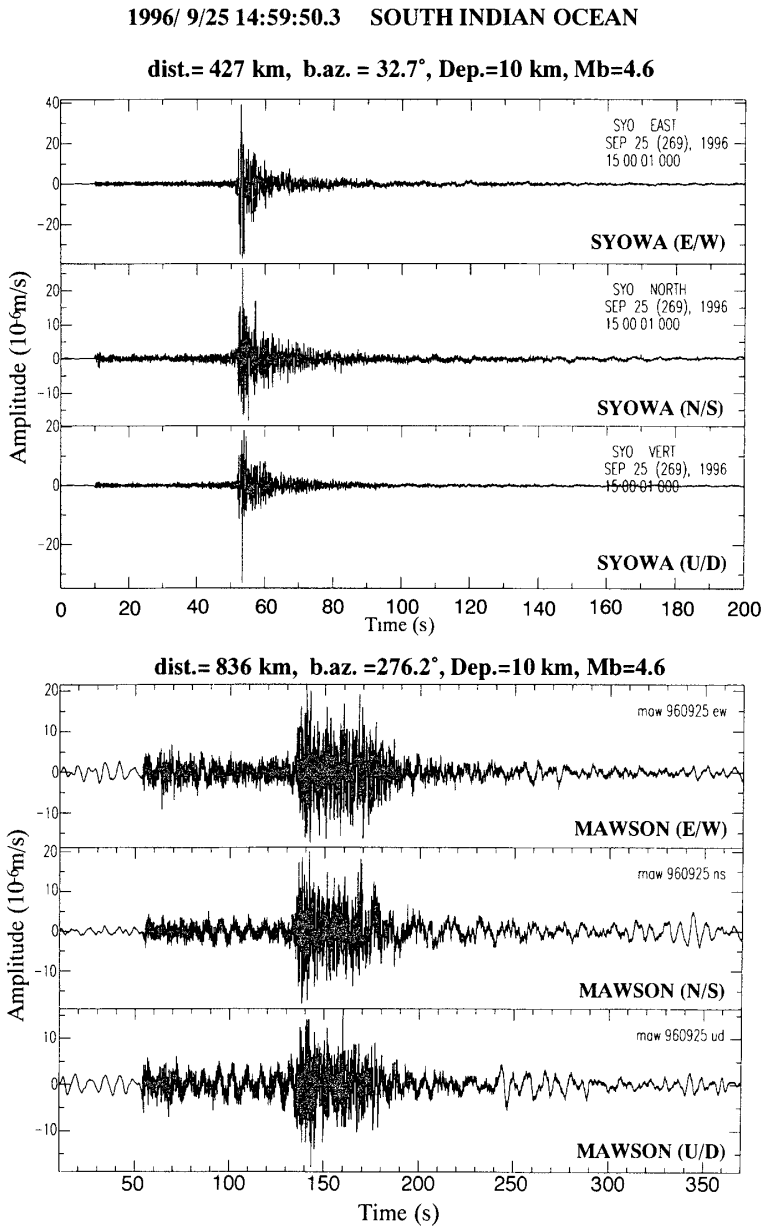

Fig. 3. Velocity waveforms of the 1996 event recorded at Syowa Station (upper plot) and Mawson Station (lower plot). The epicentral distance (dist.) and the azimuth from the station to the event (b.az.) are also shown.

As these seismometers have broadband frequency range, wide dynamic-range and high sensitivity, records of these instruments are very suitable for waveform analysis. The output signals of the seismometers at both stations are digitized at a sampling frequency of 20 Hz with a dynamic-range of 16 bits and recorded continuously. Figure 3 shows the velocity seismograms recorded at both stations. The direct *P*- and *S*-phases are clearly observed but surface waves and other converted phases cannot be seen. These waveforms are band-pass filtered with cutoff frequencies of 0.06 and 0.3 Hz, deconvolved by the responses of the seismometers, and integrated to the displacement traces. To save computational time, the seismic data were re-sampled at a rate of 10

samples per second. The displacement waveforms and their amplitudes were used for the inversion.

2.2. Moment tensor inversion by using broadband data

The focal mechanism solution of earthquakes is one of the fundamental parameters that describes the source characteristics and the stress field around the focal area. The focal mechanism is represented by the kinematic source parameters: strike, dip and rake angles. These angles have been determined mainly from the *P*-wave first motion polarities classically. However, the method needs many observations from spatially uniform coverage of stations and clear short period waveforms. Therefore, the method cannot be applied to the September 1996 event. On the other hand, the inversion method using surface waves and teleseismic long-period body waves has been greatly improved since the 1980s (*e.g.* KIKUCHI and KANAMORI, 1991). The method has been likewise successfully applied to many teleseismic earthquakes recorded by sparse networks or even by a single station (*e.g.* EKSTROM *et al.*, 1986). The optimal solution is quantitatively determined by minimizing the error between the observed and the theoretically synthesized seismograms. The method has been applied to only large events (roughly greater than M 5.5) because computation of the Green's function was difficult for shorter-period waveforms. But recently the moment tensor solution of earthquakes with magnitude less than 4.0 can be determined by using various short- or moderate-period body waves recorded by mainly the high quality broadband sensors, owing to the improvement of computer capabilities. This method, therefore, is the most suitable method applicable to Antarctic events that have recorded well only on two stations.

To calculate the moment tensor using this method, the following steps were taken. A point source was assumed for the event because the wavelengths of the major phases were far greater than the source size. In the calculation of the impulse response of the structure, one-dimensional structure was used. This one-dimensional model includes the variation of both velocities and Q-values for *P*-waves and *S*-waves, and density. The velocity model was assumed by referring to the study by IKAMI *et al.* (1984), and the Q values were assumed by referring to the Qs-model at the frequency of 4 Hz obtained by KANAO and AKAMATSU (1995) (Fig. 4). The Green's function was calculated by the wavenumber integration method (TAKEO, 1987). The moment tensor inversion was carried out by assuming a triangular source time function and a double-couple mechanism. The source process is expected to be simple because the event has a relatively small magnitude. The duration width of source time function that is twice the rise time was determined by trial and error with reference to the pulse width of the displacement trace observed at Syowa Station. The later phases are useful for the inversion using data from only a few stations. We used, however, only the body-wave parts (the direct *P*-phase and the direct *S*-phase) for the inversion. No other phase, such as *P*-coda or later phase, was used since the assumed one-dimensional model is simple and may not reflect the actual heterogeneous structure. The later part of the data was not used for the inversion because no surface wave could be identified, probably because the magnitude of this event was not so big. The surface amplification factor is fixed at 2.0 by taking only the free-surface effect into account.

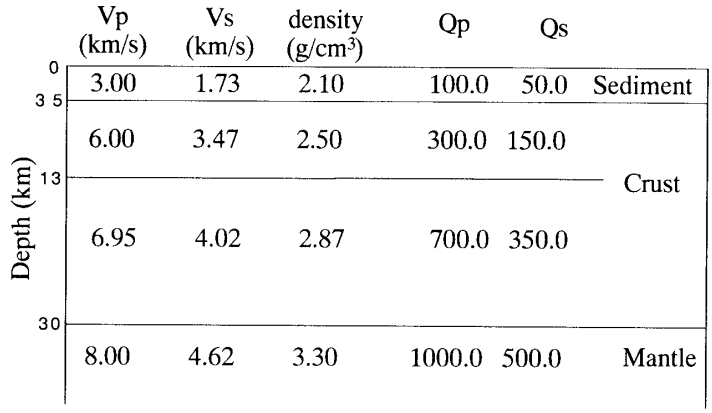

Fig. 4. The crust and the uppermost mantle model used for computing the Green's function. Vp structure is based on IKAMI *et al. (1984) with an additional sedimentary layer. Vs and density structure are estimated from Vp, and Q values are taken from the coda-Q structure in this region (*KANAO *and* AKAMATSU*, 1995).*

3. Result of Analysis

The obtained source mechanism from the inversion, the assumed source time function and the total moment value are shown in Fig. 5. The focal mechanism is plotted on the lower hemisphere of the equal-area projection, the dotted quadrants represent the compressional *P*-wave first motions. The source mechanism indicates north-south compressional strike-slip faulting with little dip-slip component. The observed and synthetic waveforms are shown in Fig. 6. These traces are normalized relative to the maximum amplitude of each trace. The maximum amplitude of each observed trace is also shown in Fig. 6. The synthetic traces correlated well with part of the observed *S*-phase waveform. However, comparison of the *P*-phases between the observed and synthetic waveforms shows a low correlation, especially for the vertical component. The low correlation is possibly due to the smaller amplitude of the vertical component compared to the horizontal component.

The mechanism of the event could be determined using the moment tensor inversion technique. However, the uniqueness of the solution has to be addressed since

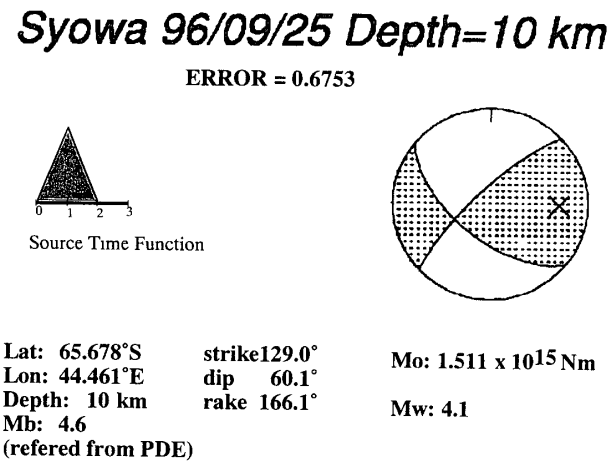

Fig. 5. The supposed source time function (left) and the resultant source mechanism solution of the inversion (right). The mechanism is plotted on the lower hemisphere of the equal area projection. The resultant source parameters are also shown.

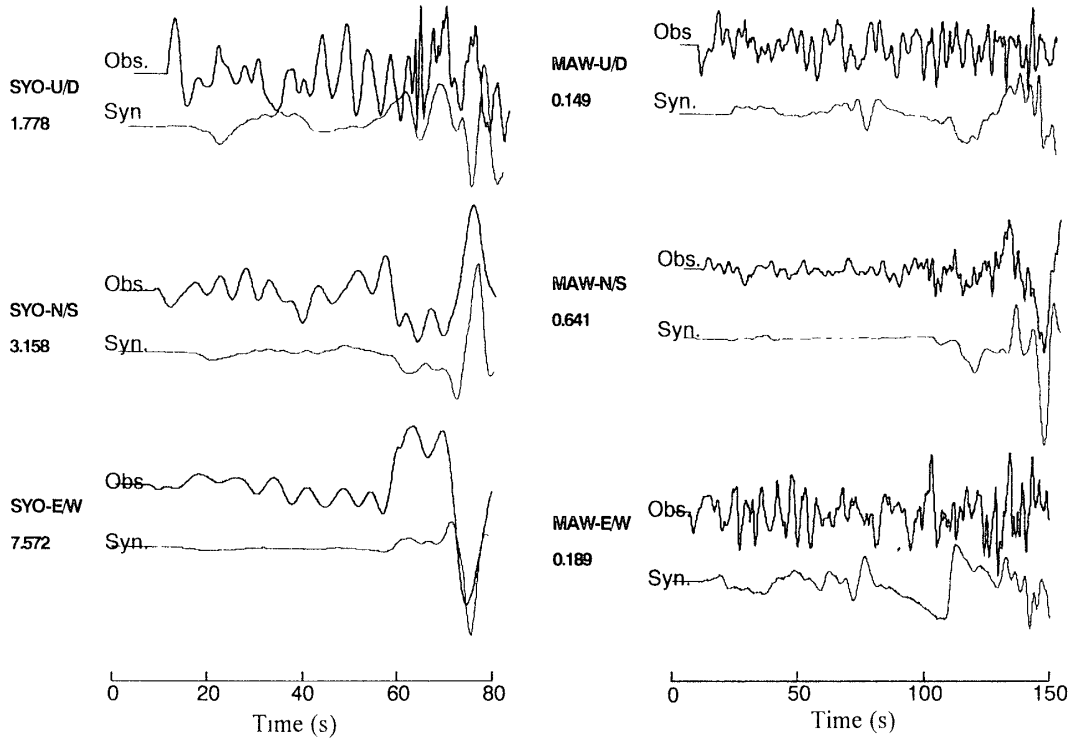

Fig. 6. Comparison between the observed data used for the inversion (upper) and synthetic waveforms (lower). The maximum amplitude of each observed trace (μm) is also shown.

there may be a limited constraint to the solution in the case of only two stations. To evaluate the uniqueness of the solution, a straightforward grid search, assuming a double-couple mechanism (WALTER, 1993), was applied to the data. During the grid search, the synthetic waveform was computed by using assumed source parameters (strike, dip, and rake angles), and the RMS error between the observed and the synthesized waveforms was calculated. The same location and the same source time function as the inversion was assumed. The search was made at 10 degree increments in strike, dip, and rake angles to find the optimal combination of the angles that produce minimum RMS error.

Figure 7 shows the "error plot diagram" (KOSUGA, 1996) on the strike-rake plane with a fixed dip angle of 60 degrees. The smallest RMS value appeared at this dip angle. White and black areas in the figure correspond to small and large RMS misfits, respectively. The pattern of error surface demonstrated in Fig. 7 is not a general one for any earthquake but a specific one that depends on the source mechanism and the relative location of source and receiver. The figure shows an elongated pattern from the upper right portion going to the lower left-hand side. These prolonged error distributions imply a trade-off between strike and rake and the existence of some local minima. Such trade-off tendencies were also shown by KOSUGA (1996). In spite of the existence of some local minima, the smallest RMS error is recognized near a strike of 130 degrees, a dip of 60 degrees and a rake of -170 degrees. This minimum is significant as compared with other local minima observed in Fig. 7. By comparing the results from the grid search and the inversion, we conclude that the result of inversion

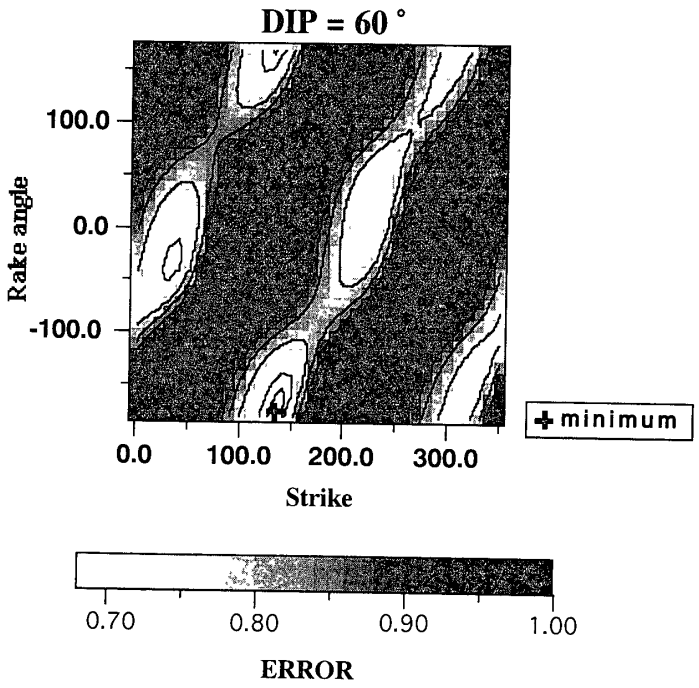

Fig. 7. The error plot diagram on the strike-rake plane with a fixed dip angle of 60°. The smallest RMS value was obtained in this dip angle. Darker shading represents larger RMS error. The cross indicates the position of minimum error.

is suitable.

4. Discussion and Summary

The inverted source mechanism is plotted on the free-air gravity anomaly map obtained from satellite altimeter missions around the epicentral region (SANDWELL and SMITH, 1992) in Fig. 8. It is considered that such gravity anomalies in the oceanic region indicate submarine topography. The figure implies that the 1996 event occurred along a lineament extending along the northwest-southeast direction. This lineament was presumed as a fracture zone on the sea floor from the investigation of magnetic anomalies (NOGI *et al.*, 1996). One of the nodal planes of the obtained mechanism is nearly parallel to this lineament. Therefore, the 1996 earthquake is possibly an event that ruptured along the sea floor lineament. If this is correct, the 1996 event may indicate activity along a remnant of an old transform fault system. The South Indian Ocean is the location of the dispersal of Gondwana fragments during the Jurassic period. The lineament, therefore, possibly indicates the direction of sea-floor spreading during the early stage of the Gondwana break-up. Moreover, the magnetic anomaly lineations usually show a NE-SW direction around this area (NOGI *et al.*, 1996). It is very interesting to note that the 1996 earthquake occurred at the fracture zone of the Antarctic plate. This is most probably an indication of the present activity of the fracture zone. The source mechanism of the 1996 event determined in this paper provides an important clue to understand not only the present tectonic but the historical development of the Antarctic plate, which is one of the essential problems still unsolved

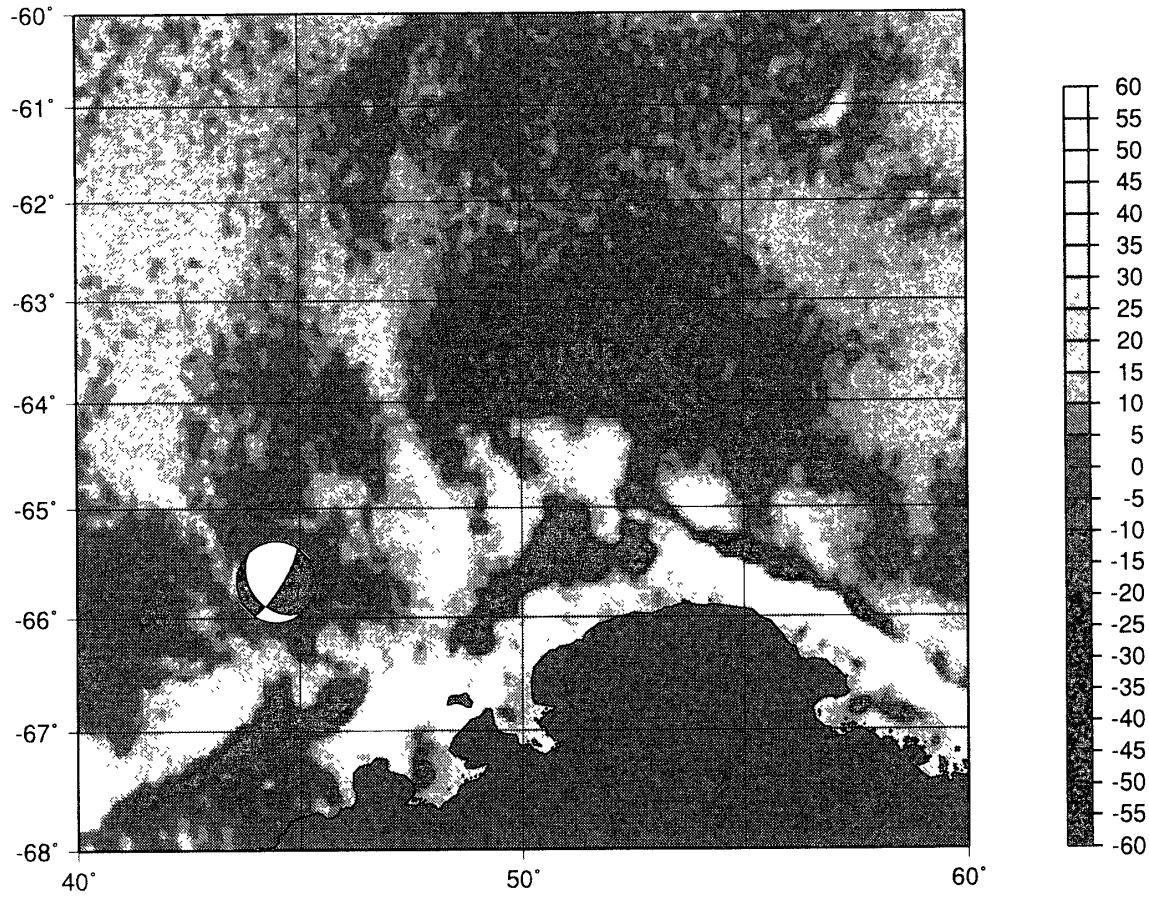

Fig. 8. Free-air gravity anomaly map around the epicentral region (after SANDWELL and SMITH, 1992). The focal mechanism of the 1996 event is also shown.

due to the lack of information about the driving force.

Acknowledgments

The authors express their thanks to Dr. M. LEONARD of the Australian Seismological Center for the providing the event data at Mawson Station, Antarctica. They also wish to thank Dr. M. KOSUGA of Hirosaki University for his program and helpful discussions. Thanks also go to Dr. A. KUBO for his valuable advice and discussions. Two anonymous referees provided thoughtful reviews, which improved the manuscript.

References

EKSTROM, G., DZIEWONSKI, A.M. and STEIN, J.M. (1986): Single station CMT; Application to the Michoacan Mexico earthquake of September 19, 1985. Geophys. Res. Lett., **13**, 173–176.

IKAMI, A., ITO, K., SHIBUYA, K. and KAMINUMA, K. (1984): Deep crustal structure along the profile between Syowa and Mizuho Stations, East Antarctica. Mem. Natl Inst. Polar Res., Ser. C (Earth Sci.), **15**, 19–28.

KAMINUMA, K. (1994): Seismic activity in and around the Antarctic Continent. Terra Antarct., **1**, 423–426.

KANAO, M. and AKAMATSU, J. (1995): Shear wave Q structure for lithosphere in the Lützow-Holm Bay region, East Antarctica. Proc. NIPR Symp. Antarct. Geosci., **8**, 1–14.

KIKUCHI, M. and KANAMORI, H. (1991): Inversion of complex body waves-III. Bull. Seismol. Soc. Am., **81**, 2335–2350.

KOSUGA, M. (1996): Near-field moment tensor inversion and stress field in northeastern Japan. Ph.D. Thesis of Tohoku University, 233 p.

NOGI, Y., SEAMA, N., ISEZAKI, N. and FUKUDA, Y. (1996): Magnetic anomaly lineations and fracture zones deduced from vector magnetic anomalies in the West Enderby Basin. Weddell Sea Tectonics and Gondwana Break-up, ed. by B.C. STOREY *et al.* London, Geological Society of London, 265–273 (Geol. Soc. Spec. Publ., 108).

OKAL, E.A. (1981): Intraplate seismicity of Antarctica and tectonic implications. Earth Planet. Sci. Lett., **52**, 397–409.

SANDWELL, D.T. and SMITH, W.H.F. (1992): Global marine gravity from ERS-1, GEOSAT and SEASAT reveals new tectonic fabric. EOS; Trans., **73**, 133.

TAKEO, M. (1987): An inversion method to analyze the rupture processes of earthquakes using near-field seismograms. Bull. Seismol. Soc. Am., **77**, 490–513.

WALTER, W.R. (1993): Source parameters of the June 29, 1992 Little Skull Mountain Earthquake from complete regional waveforms at a single station. Geophys. Res. Lett., **20**, 403–406.

WIELANDT, E. and STRECKEISEN, G. (1982): The leaf-spring seismometer: Design and performance. Bull. Seismol. Soc. Am., **72**, 2349–2367.

(Received March 20, 1998; Revised manuscript accepted June 16, 1998)